

# Adsorption of Fluorinated Ethers and Alcohols on Graphite

Nisha Shukla

Seagate Research Center, Pittsburgh, Pennsylvania 15203

Jing Gui

Seagate Technology, Inc., Fremont, California 94538

Andrew J. Gellman\*

Department of Chemical Engineering, Carnegie Mellon University,  
Pittsburgh, Pennsylvania 15213

Received October 2, 2000. In Final Form: January 29, 2001

As part of a research program to determine the nature of the interactions of perfluoropolyalkyl ether lubricants with the surfaces of magnetic data storage media, we have studied the desorption of several model compounds from the surface of graphite. In this instance we have been modeling the chemical functionality of the lubricant Fomblin Zdol by using perfluorodiethyl ether ((CF<sub>3</sub>CF<sub>2</sub>)<sub>2</sub>O) to represent the ether linkages of its backbone and 2,2,2-trifluoroethanol (CF<sub>3</sub>CH<sub>2</sub>OH) to represent its hydroxyl end groups. The desorption kinetics of these compounds from the basal plane of graphite have been compared with those of their hydrocarbon analogues (CH<sub>3</sub>CH<sub>2</sub>)<sub>2</sub>O and CH<sub>3</sub>CH<sub>2</sub>OH. More importantly, the desorption of these compounds from graphite has been compared with prior measurements of their desorption from numerous types of amorphous carbon films. The desorption from graphite occurs with zero-order kinetics and well-defined desorption energies. The results of these measurements indicate that the broad distributions of desorption energies observed on amorphous carbon films are due to heterogeneity of the carbon films rather than lateral interactions between adsorbed species. The nature of the interactions of the ethers and alcohols with the graphite surface is consistent with previously proposed models for the interactions of fluorinated ethers and fluorinated alcohols with amorphous carbon films.

## 1. Introduction

Magnetic data storage media require protection from the read–write heads that fly over their surfaces at heights of <200 Å and speeds of several meters per second. As continued increases are made in the density of data stored on these surfaces, the gap between the media and the read–write head decreases, thereby increasing the performance required of the protecting layers. These layers are usually composed of a thin coating (<100 Å) of amorphous carbon (a-C) and an even thinner film (<20 Å) of perfluoropolyalkyl ether (PFPE) lubricant.<sup>1–3</sup> The performance of the lubricant–overcoat combination depends on the properties of the lubricant in contact with the a-C film and thus the surface chemistry of the lubricant on the carbon. The results presented in this paper shed some light on various aspects of this surface chemistry.

There have been a number of studies of various aspects of the surface chemistry of PFPE lubricants on a-C films. These have focused on such properties as thermal stability, chemical decomposition, wetting of the lubricant onto the surface, and bonding of the lubricant to the a-C film.<sup>4–10</sup>

The work from our laboratory has focused on determining the nature of the chemical interactions of the lubricant with the carbon film and the effects of film composition on these interactions.<sup>11–16</sup> The most common of the PFPE lubricants is Fomblin Zdol, which consists of a perfluorinated ether backbone terminated at either end by hydroxyl groups.



The carbon films used for or considered for use in magnetic data storage include hydrogenated carbons (a-CH<sub>x</sub>), nitrogenated carbon (a-CN<sub>x</sub>), diamond-like carbon (DLC), and other forms. To understand the nature of the interactions of a complex molecule such as Fomblin Zdol

\* To whom correspondence should be addressed.

(1) Bhushan, B. *Tribology and Mechanics of Magnetic Storage Devices*, 2nd ed.; Springer-Verlag: New York, 1996.

(2) Mate, C. M.; Homola, A. M. In *Molecular Tribology of Disk Drives*; Bhushan, B., Ed.; Kluwer Academic Publishers: Netherlands, 1997; p 647.

(3) Gellman, A. J. *Curr. Opin. Colloid Interface Sci.* **1998**, 3(4), 368.

(4) Lin, J.-L.; Bhatia, C. S.; Yates, J. T. *J. Vac. Sci. Technol.* **1995**, A13(2), 163.

(5) Strom, B. D.; Bogy, D. B.; Bhatia, C. S.; Bhushan, B. *J. Tribol.* **1991**, 113, 689.

(6) Dai, Q.; Vurens, G.; Luna, M.; Salmeron, M. *Langmuir* **1997**, 13, 4401.

(7) Waltman, R. J.; Packer, D. J.; Tyndall, G. W. *Tribol. Lett.* **1998**, 4(3–4), 267.

(8) Ruhe, J.; Novotny, V.; Clarke, T.; Street, G. B. *J. Tribol.* **1996**, 118, 663.

(9) Wang, R. H.; White, R. L.; Meeks, S. W.; Min, B. G.; Kellock, A.; Homola, A.; Yoon, D. *IEEE Trans. Magn.* **1997**, 33, 926.

(10) O'Connor, T. M.; Back, Y. R.; Jhon, M. S.; Min, B. G.; Yoon, D. Y.; Karis, T. E. *J. Appl. Phys.* **1996**, 79(8), 5788.

(11) Cornaglia, L.; Gellman, A. J. *J. Vac. Sci. Technol.* **1997**, A15(5), 2755.

(12) Cornaglia, L.; Gellman, A. J. *Adv. Info. Stor. Sys.* **1998**, 8, 57.

(13) Paserba, K.; Shukla, N.; Gellman, A. J.; Gui, J.; Marchon, B. *Langmuir* **1999**, 15(5), 1709.

(14) Lei, R. Z.; Gellman, A. J. *Langmuir* **2000**, 16(16), 6628.

(15) Shukla, N.; Gellman, A. J.; Gui, J. *Langmuir* **2000**, 16(16), 6562.

(16) Shukla, N.; Gellman, A. J. *J. Vac. Sci. Technol.*, in press.

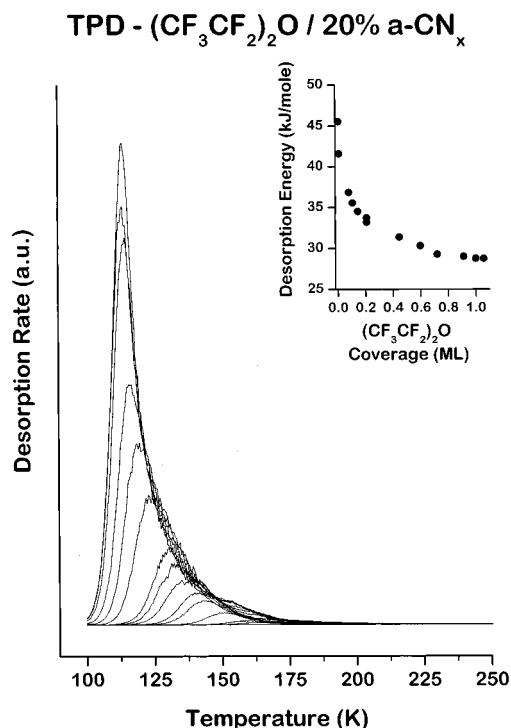


**Figure 1.** Thermal desorption spectra of  $(\text{CF}_3\text{CF}_2)_2\text{O}$  from the surface of an a-CN<sub>x</sub> film. The initial coverage of the  $(\text{CF}_3\text{CF}_2)_2\text{O}$  varies from <1% of a monolayer to 1 ML. The peak desorption temperatures are decreasing with increasing coverage. The TPD spectra were collected with a heating rate of 2 K/s while monitoring the signal at  $m/q = 69$ . The inset shows the desorption energy versus coverage calculated from the desorption peak temperatures.

with the surfaces of a-C films, we have studied separately the adsorption of fluorinated ethers and fluorinated alcohols on a wide variety of a-C films.<sup>15</sup> These molecules independently model the linkages of the ether backbone and the hydroxyl end groups of Fomblin Zdol.

The experimental approach of previous studies of ether adsorption on the a-C films has involved the measurement of the desorption kinetics and desorption energies of a number of fluorinated ethers and their hydrocarbon analogues. An example of the TPD spectra of perfluoro-diethyl ether ( $(\text{CF}_3\text{CF}_2)_2\text{O}$ ) on an a-CN<sub>x</sub> film is shown in Figure 1. As the coverage increases, the peak desorption temperature decreases smoothly toward that associated with the desorption of the condensed multilayer. The peaks are very broad, and there is no clear resolution of the monolayer and the multilayer desorption features. To interpret these spectra, we have made the assumption that the desorption process is first-order with a coverage dependent desorption energy.

$$r = \nu \exp(-\Delta E(\theta)/RT) \times \theta$$

With the assumption that the pre-exponent is  $\nu = 10^{13} \text{ s}^{-1}$  the desorption energy has been estimated and is plotted as a function of coverage in the inset to Figure 1.<sup>15</sup> Comparison of the desorption energies of the fluorinated ethers with those of their hydrocarbon analogues shows that fluorination always lowers the desorption energy, independent of the type of a-CH<sub>x</sub> or a-CN<sub>x</sub> film or the type of ether.<sup>11–13</sup> The implication of this observation is that the ethers bond to the surface by electron donation from the lone pair electrons on the oxygen atoms of the ether linkage.

In a manner similar to the study of the ethers, we have also compared the desorption of fluorinated alcohols and

their hydrocarbon analogues on a-C films.<sup>13,16</sup> The basic features of the desorption spectra for the alcohols are similar to those observed for the ethers in the sense that the desorption peaks are broad, the peak desorption temperature decreases with increasing coverage, and there is no clear resolution of the monolayer and multilayer desorption features. Again, this has been interpreted to imply that there are a variety of alcohol binding sites on the surfaces of a-C films. In all cases though, the desorption energy of the fluorinated alcohols is higher than the desorption energy of the hydrocarbon alcohols. The implication of this observation is that the alcohols interact with the a-C surfaces via hydrogen bonding.

All thermal desorption spectra of the ethers and alcohols on a-C films have exhibited the basic features illustrated by the desorption spectra in Figure 1. Among the molecules studied, they differ only in the exact peak temperatures and the ranges of desorption temperatures. The primary feature alluded to earlier that complicates the interpretation of those desorption spectra is that the peak desorption temperature decreases with increasing adsorbate coverage. For a first-order desorption process, which this ought to be, this implies that the desorption energy is decreasing with increasing coverage. One of the possible causes of this decrease is that there are repulsive lateral interactions between the adsorbates on the surface. This seems unlikely, given previous experience studying the desorption of these molecules from the Cu(111) surface.<sup>17</sup> On that surface which is single crystalline and homogeneous the desorption spectra for the fluorinated ethers reveal that, if anything, the interactions between the adsorbed molecules are attractive. This has also been observed on other single-crystal metal surfaces.<sup>18–20</sup> A second possible cause of the coverage dependent desorption features observed on the a-C films is that their surfaces are heterogeneous and expose a variety of binding sites with a range of different affinities for the adsorption of the ethers and the alcohols. At low coverages the adsorbed molecules populate those sites with the highest binding affinities and then sequentially populate sites with lower and lower affinities until the surface is saturated and the formation of the second and third layers begins. This scenario seems reasonable given that the films are known to be composed of a mixture of  $\text{sp}^2$  and  $\text{sp}^3$  hybridized carbon atoms and there is ample evidence for the presence of a variety of different partially oxidized species at the surface.<sup>15,21</sup> The intent of the work presented in this paper is to address the issue of whether the coverage dependent desorption energies observed in previous work are due to adsorbate–adsorbate interactions or to heterogeneity of the a-C film surface.

The experiments reported in this paper have measured the desorption kinetics of ethers and alcohols adsorbed on the basal plane of graphite. This surface is pure carbon and thus bears some compositional relationship to the a-C films used for protection of data storage media but is single crystalline and homogeneous. The graphite surface differs from the a-C films in that it consists of purely  $\text{sp}^2$  hybridized carbon and has no partially oxidized groups. As a result the desorption data that can be obtained from this surface allow an unambiguous determination of

(17) Meyers, J. M.; Street, S. C.; Thompson, S.; Gellman, A. J. *Langmuir* **1996**, *12* (6), 1511.

(18) Jenks, C. J.; Joyce, J. A.; Thiel, P. A. *J. Vac. Sci. Technol.* **1994**, *A12* (4), 2101.

(19) Walczak, M. M.; Thiel, P. A. *Surf. Sci.* **1989**, *224*, 425.

(20) Walczak, M. M.; Leavitt, P. K.; Thiel, P. A. *Trib. Trans.* **1990**, *33* (4), 557.

(21) Yanagisawa, M. *Tribol. Mech. Magn. Stor. Sys., STLE Publ.* **1994**, *9*, 36.

desorption energies and pre-exponential factors. At the same time they reveal that the natural interactions between adsorbed ethers or between adsorbed alcohols are attractive rather than repulsive. The implication is that the coverage dependence of the desorption energies on the a-C films is due to heterogeneity of the surface and the presence of a variety of types of binding sites.

## 2. Experimental Section

The experiments were carried out in a stainless steel ultrahigh vacuum chamber evacuated by a cryopump and a titanium sublimation pump to a base pressure of  $4 \times 10^{-11}$  Torr. The chamber was equipped with two leak valves with 3/8 in. diameter stainless steel dosing tubes for introducing the alcohol and ether vapors into the chamber for adsorption onto the graphite surface. In addition the system was equipped with low-energy electron diffraction (LEED) optics. The thermally programmed desorption (TPD) experiment used an Ametek Dycor MA200M quadrupole mass spectrometer which allowed five  $m/q$  ratios to be recorded simultaneously.

The single-crystal pyrolytic graphite sample (grade ZYA) used in this work was obtained from Advanced Ceramics Corporation. The dimensions of the graphite sample were 12 mm  $\times$  12 mm  $\times$  2 mm. The sample was clipped onto a tantalum foil slightly larger than the sample itself, and the foil was spot-welded using tantalum wire onto the end of the UHV sample manipulator. The graphite sample was cleaned by first peeling off a layer of graphite and then heating to 1000 K under vacuum. A LEED pattern of graphite showed sharp bright spots although the pattern was not that of a perfect hexagonal lattice and suggested the presence of several single-crystalline domains at the surface. Uniform heating of the sample was tested by heating the sample and visually ascertaining that the wires and Ta foil used to mount the sample glowed with uniform color. Furthermore, the extremely narrow peaks observed in thermal desorption spectra demonstrate that sample heating was quite uniform.

No cleaning of the graphite surface was required other than annealing to desorb physisorbed species. None of the species used are expected to react with the basal plane of graphite, and the extremely high reproducibility of the desorption spectra throughout the entire time used to collect the data attests to the fact that the surface is very inert and remains extremely clean during these experiments. To obtain the thermal desorption spectra, the surface was first cooled in a vacuum to <90 K. The alcohols and ethers were adsorbed onto the surface by introduction of their vapors into the background vacuum at controlled pressures and for controlled time periods. After exposure to the adsorbate vapor the surface was positioned in front of the aperture to the mass spectrometer and heated at a constant rate of 2 K/s under computer control. During heating the mass spectrometer was used to collect signals for up to five  $m/q$  ratios of the desorbing species. In no case was there any indication of reaction of the adsorbate on the surface. All four adsorbates adsorbed and desorbed reversibly.

Ethanol ( $\text{CH}_3\text{CH}_2\text{OH}$ , 99.5%) was purchased from Aldrich Chemicals. 2,2,2-Trifluoroethanol ( $\text{CF}_3\text{CH}_2\text{OH}$ , 99.5%) was purchased from Lancaster Chemicals. Diethyl ether ( $(\text{CH}_3\text{CH}_2)_2\text{O}$ , 99%) was purchased from Aldrich Chemicals, and perfluorodiethyl ether ( $(\text{CF}_3\text{CF}_2)_2\text{O}$ , 99%) was purchased from PCR. All chemicals except perfluorodiethyl ether were purified using several cycles of freeze-pump-thawing. Perfluorodiethyl ether is a gas and was used as provided. The purity of all chemicals was checked by mass spectrometry.

## 3. Results

**3.1. Ether Desorption from Graphite.** The ether linkages in the main chain of Fomblin Zdol have been modeled in this work by the use of  $(\text{CF}_3\text{CF}_2)_2\text{O}$ . The desorption spectra of  $(\text{CF}_3\text{CF}_2)_2\text{O}$  from the graphite surface are shown in Figure 2 for a range of different initial coverages. It is obvious that these are substantially different from those shown in Figure 1 for desorption from an a- $\text{CN}_x$  film. At low coverage (<1% of a monolayer) there

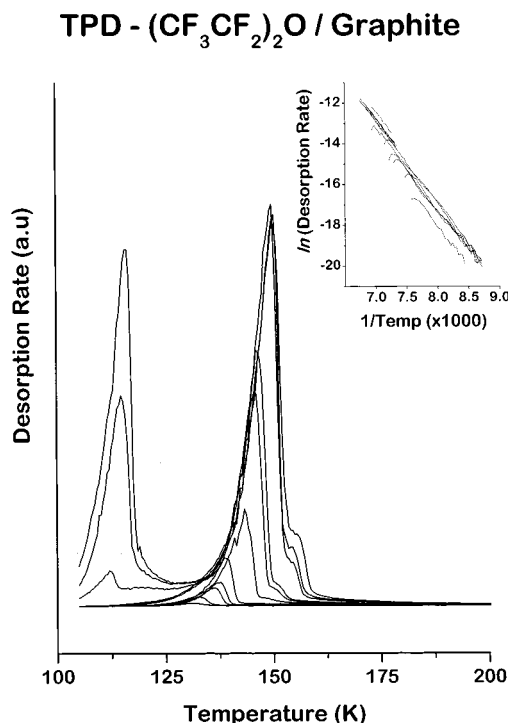


**Figure 2.** Thermal desorption of  $(\text{CF}_3\text{CF}_2)_2\text{O}$  from the surface of graphite. The initial  $(\text{CF}_3\text{CF}_2)_2\text{O}$  coverage ranges from <1% to >1 ML. The monolayer and multilayer desorption features are now quite well resolved, and the peak desorption temperatures for the monolayer increase with increasing coverage. The TPD spectra were collected with a heating rate of 2 K/s while monitoring the signal at  $m/q = 69$ . The inset shows an Arrhenius plot of the leading edges of the monolayer desorption curves. The straight lines indicate that the process is zero-order, and the slopes give a desorption energy of  $\Delta E_{\text{des}} = 32.5 \pm 0.9$  kJ/mol.

is a single desorption peak at 131 K. As the coverage is increased, this peak grows in intensity until it saturates with the peak position at 150 K. This high-temperature desorption feature is attributed to the desorption of the adsorbed monolayer on the graphite surface. Once this peak has saturated in intensity, a second desorption feature appears at 112 K. This also increases in intensity with increasing coverage but appears to grow without bound and is attributed to desorption from a multilayer film of  $(\text{CF}_3\text{CF}_2)_2\text{O}$  on the graphite surface.

Comparison with the spectra in Figure 1 shows that the widths of the monolayer desorption curves on the graphite surface ( $\Delta T \sim 7$  K) are far smaller than those on the a- $\text{CH}_x$  film ( $\Delta T \sim 30$  K). Furthermore, on the graphite surface the peaks shift to higher temperature rather than lower temperature with increasing coverage and there is a well-defined transition with coverage from a monolayer desorption regime to a multilayer desorption regime. The implication of this behavior is that the interactions between the adsorbed  $(\text{CF}_3\text{CF}_2)_2\text{O}$  are attractive in nature, and this is apparent on the graphite surface because of the homogeneity of the surface. The desorption behavior also implies that the shift to lower temperatures of the desorption peaks on the a- $\text{CN}_x$  film is due to heterogeneity of its surface, which masks the naturally attractive interactions between the adsorbed  $(\text{CF}_3\text{CF}_2)_2\text{O}$ .

The last feature to note concerning the  $(\text{CF}_3\text{CF}_2)_2\text{O}$  desorption spectra on the graphite surface is that they have rapidly rising leading edges that tend to line up over one another and that following the peak the decrease in the desorption rate is extremely rapid. This behavior is classically indicative of a zero-order desorption phenom-

**Table 1. Desorption Energies and Pre-exponential Factors Observed on the Graphite Surface**

adsorbate	$\Delta E_{\text{des}}$ (kJ/mol)	$\nu$ ( $\text{s}^{-1}$ )
$(\text{CF}_3\text{CF}_2)_2\text{O}$	$32.5 \pm 0.9$	$7.6 (\pm 2.2) \times 10^{10}$
$(\text{CH}_3\text{CH}_2)_2\text{O}$	$45.4 \pm 1.8$	$8.1 (\pm 1.2) \times 10^{13}$
$\text{CF}_3\text{CH}_2\text{OH}$	$55.9 \pm 0.9$	$7.6 (\pm 2.1) \times 10^{15}$
$\text{CH}_3\text{CH}_2\text{OH}$	$57.6 \pm 0.7$	$7.6 (\pm 1.3) \times 10^{16}$

enon with a rate expression of the form

$$r = k\theta^0 = \nu \exp(-\Delta E_{\text{des}}/RT)$$

This is demonstrated by the inset of Figure 2, which plots  $\ln(r)$  versus  $1/T$  for the leading edges of all the spectra. It is quite clear that these yield straight lines all the way to the peak of the desorption feature. The rationale for this behavior will be discussed below. The important point is that the slopes of these lines give the desorption energy ( $\Delta E_{\text{des}}$ ) without the need for a pre-exponential factor, as would be the case for a first-order desorption process. The pre-exponential factor can then be determined independently. In this case the desorption energy for  $(\text{CF}_3\text{CF}_2)_2\text{O}$  on the graphite surface is  $\Delta E_{\text{des}} = 32.5 \pm 0.9$  kJ/mol. This falls into the range of desorption energies estimated for  $(\text{CF}_3\text{CF}_2)_2\text{O}$  on the a-C films.<sup>11–13</sup>

The pre-exponential factor for the desorption rate constant can be determined from the expression

$$\nu = \beta \theta_0 \int_0^{T_m} \exp(-\Delta E_{\text{des}}/RT) dT^{-1}$$

where  $\theta_0$  is the initial coverage of the adsorbate relative to the saturated monolayer,  $\beta$  is the heating rate, and  $T_m$  is the temperature of the peak maximum in the desorption spectrum. Using this expression, the pre-exponential for  $(\text{CF}_3\text{CF}_2)_2\text{O}$  desorption from graphite has been estimated from all the desorption peaks to be  $\nu = (7.7 \pm 2.2) \times 10^{10} \text{ s}^{-1}$ . The desorption energies and pre-exponential factors measured for all molecules adsorbed on graphite have been summarized in Table 1.

In previous work it has been instructive to compare the desorption energies of the fluorinated ethers with those of their hydrocarbon analogues in order to probe the nature of the interactions with the a-C films. This has been done in this investigation by studying the desorption spectra of  $(\text{CH}_3\text{CH}_2)_2\text{O}$  on the graphite surface. These are shown in Figure 3, and it is immediately obvious that they exhibit the same basic behavior as that of the desorption spectra of  $(\text{CF}_3\text{CF}_2)_2\text{O}$ . The only real difference is that monolayer desorption features appear in the temperature range 151–166 K, higher than those observed for the desorption of the  $(\text{CF}_3\text{CF}_2)_2\text{O}$ . The inset in the top right corner of Figure 3 is an Arrhenius plot which reveals that the desorption behavior is a zero-order process. The straight-line Arrhenius fits to the monolayer desorption curves give  $\Delta E_{\text{des}} = 45.4 \pm 1.8$  kJ/mol for  $(\text{CH}_3\text{CH}_2)_2\text{O}$  on the graphite surface. This is significantly higher than that observed for  $(\text{CF}_3\text{CF}_2)_2\text{O}$ , which is entirely consistent with our observations on the a-C films.<sup>11–13</sup> On those surfaces the values of  $\Delta E_{\text{des}}$  for  $(\text{CH}_3\text{CH}_2)_2\text{O}$  in the low-coverage limit were  $\sim 52$  kJ/mol and were 6–11 kJ/mol higher than those of  $(\text{CF}_3\text{CF}_2)_2\text{O}$  on the same a-C surfaces. The pre-exponential factor for  $(\text{CH}_3\text{CH}_2)_2\text{O}$  desorption from the graphite surface was determined to be  $\nu = (8.1 \pm 1.2) \times 10^{13} \text{ s}^{-1}$ .

In principle the desorption energetics of condensed multilayers on any surface should not be influenced by the substrate and should reflect the heat of vaporization of the condensed phase of the adsorbate. It has been

### TPD - $(\text{CH}_3\text{CH}_2)_2\text{O}$ / Graphite

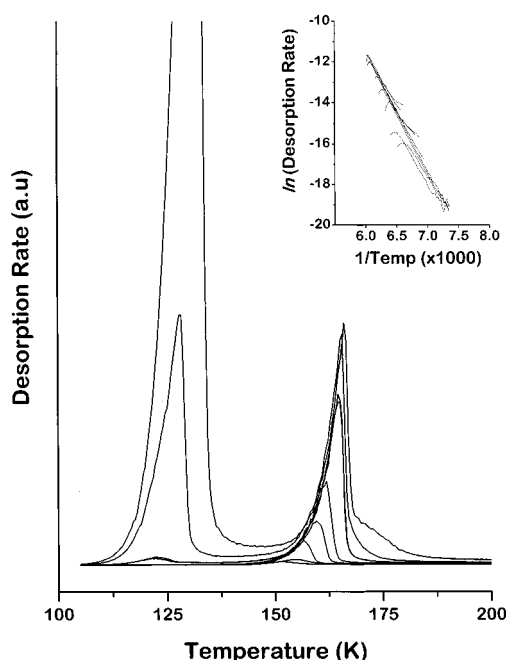


**Figure 3.** Thermal desorption of  $(\text{CH}_3\text{CH}_2)_2\text{O}$  from the surface of graphite. The initial  $(\text{CH}_3\text{CH}_2)_2\text{O}$  coverage ranges from  $<1\%$  to  $>5$  ML. The monolayer and multilayer desorption features are well resolved, and the peak desorption temperatures for the monolayer increase with increasing coverage. The TPD spectra were collected with a heating rate of 2 K/s while monitoring the signal at  $m/q = 29$ . The inset shows an Arrhenius plot of the leading edges of the monolayer desorption curves. The straight lines indicate that the process is zero-order, and the slopes give a desorption energy of  $\Delta E_{\text{des}} = 45.4 \pm 1.8$  kJ/mol. Note that this is substantially higher than that for  $(\text{CF}_3\text{CF}_2)_2\text{O}$ .

possible to obtain a value for the desorption energy of the  $(\text{CH}_3\text{CH}_2)_2\text{O}$  multilayer on graphite using the same type of analysis as has been used for the zero-order desorption of the adsorbed monolayer. This yields a value of  $\Delta E_{\text{des}}^{\text{mult}} = 32.9 \pm 1.2$  kJ/mol. This can be compared with the prediction from experimental data for the  $\Delta H_{\text{vap}}$  collected in the temperature range 281–313 K.<sup>22</sup> When this correlation is used to estimate the  $\Delta H_{\text{vap}}$  of  $(\text{CH}_3\text{CH}_2)_2\text{O}$  at 125 K (the multilayer desorption temperature), it yields  $\Delta H_{\text{vap}} = 36.6$  kJ/mol, which is quite close to the value of  $\Delta E_{\text{des}}^{\text{mult}}$  estimated from the multilayer desorption spectra.

**3.2. Desorption of Alcohols from Graphite Surfaces.** The alcohols have been used to model the end groups of Fomblin Zdol and their interactions with a-C surfaces.<sup>13,16</sup> In this work we have used  $\text{CF}_3\text{CH}_2\text{OH}$  and measured its desorption kinetics from the surface of graphite. Figure 4 shows the TPD spectra of  $\text{CF}_3\text{CH}_2\text{OH}$  from the graphite surface. The basic behavior of the desorption process is similar to that observed for the desorption of the ethers. A monolayer peak is populated at low coverages and exhibits zero-order desorption kinetics. It is well resolved from the multilayer desorption feature. The inset reveals the Arrhenius behavior of the monolayer desorption feature and indicates that  $\Delta E_{\text{des}} = 59.0 \pm 4.2$  kJ/mol. The accuracy of this number is not quite as good as that for the ethers, and this is probably because a number of the spectra exhibit some overlap of

(22) Majer, V.; Svoboda, V. *Enthalpies of Vaporization of Organic Compounds: A Critical Review and Data Compilation*; Blackwell Scientific Publications: Oxford, 1985; p 300.

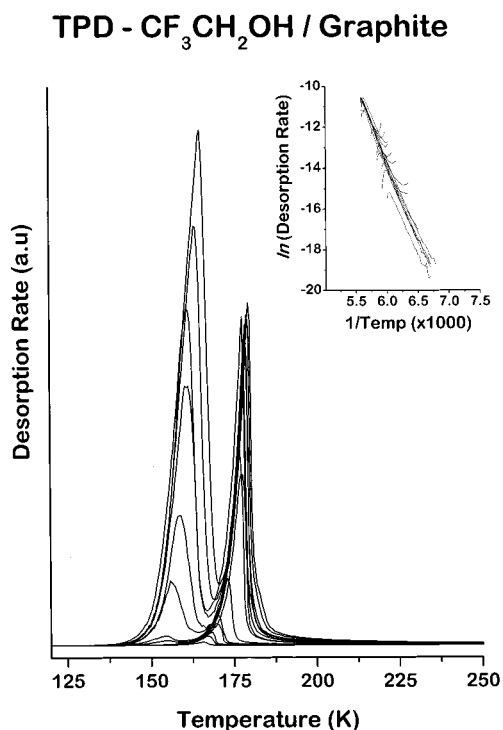


**Figure 4.** Thermal desorption of CF<sub>3</sub>CH<sub>2</sub>OH from the surface of graphite. The initial CF<sub>3</sub>CH<sub>2</sub>OH coverage ranges from <1% to >2 ML. The monolayer and multilayer desorption features are well resolved, although there is some overlap at high coverages. The monolayer peak desorption temperatures increase with increasing coverage. The TPD spectra were collected with a heating rate of 2 K/s while monitoring the signal at  $m/q = 31$ . The inset shows an Arrhenius plot of the leading edges of the monolayer desorption curves. The straight lines indicate that the process is zero-order, and the slopes give a desorption energy of  $\Delta E_{\text{des}} = 55.9 \pm 0.9$  kJ/mol.

the multilayer desorption tail with the leading edge of the monolayer desorption feature. This is not important from the point of this paper, but if those spectra which include multilayer desorption are not included in the calculation, then the desorption energy is reduced slightly to  $\Delta E_{\text{des}} = 55.9 \pm 0.9$  kJ/mol. This is the number that will be used for future discussion. Both these values fall into the range of desorption energies estimated on the a-C films at low CF<sub>3</sub>CH<sub>2</sub>OH coverages. The desorption pre-exponent has been determined to be  $\nu = (7.6 \pm 2.1) \times 10^{15} \text{ s}^{-1}$ .

The desorption of CH<sub>3</sub>CH<sub>2</sub>OH was compared with that of CF<sub>3</sub>CH<sub>2</sub>OH in previous work in order to probe the nature of the bonding of the hydroxyl end groups of Fomblin Zdl to a-C surfaces.<sup>13–16</sup> Figure 5 shows the desorption spectra for CH<sub>3</sub>CH<sub>2</sub>OH on the graphite surface. Again the same basic features are observed for CH<sub>3</sub>CH<sub>2</sub>OH desorption as for the desorption of CF<sub>3</sub>CH<sub>2</sub>OH. The monolayer desorption energy predicted using all the curves in the inset is  $\Delta E_{\text{des}} = 60.9 \pm 3.9$  kJ/mol. Once again the accuracy of this number may be influenced by the overlap of the multilayer and monolayer desorption features. If one ignores those spectra for which there is overlap, the desorption energy for ethanol on the graphite surface is reduced to  $\Delta E_{\text{des}} = 57.6 \pm 0.7$  kJ/mol. The pre-exponential factor was determined to be  $\nu = (7.6 \pm 1.3) \times 10^{16} \text{ s}^{-1}$ . Note that the  $\Delta E_{\text{des}}$  is not significantly different from that found for CF<sub>3</sub>CH<sub>2</sub>OH desorption from graphite. This is a departure from what has been observed in the past for CF<sub>3</sub>CH<sub>2</sub>OH and CH<sub>3</sub>CH<sub>2</sub>OH adsorption on the a-C surfaces. In those cases the desorption energies for CF<sub>3</sub>CH<sub>2</sub>OH were always observed to be higher than those of CH<sub>3</sub>CH<sub>2</sub>OH.

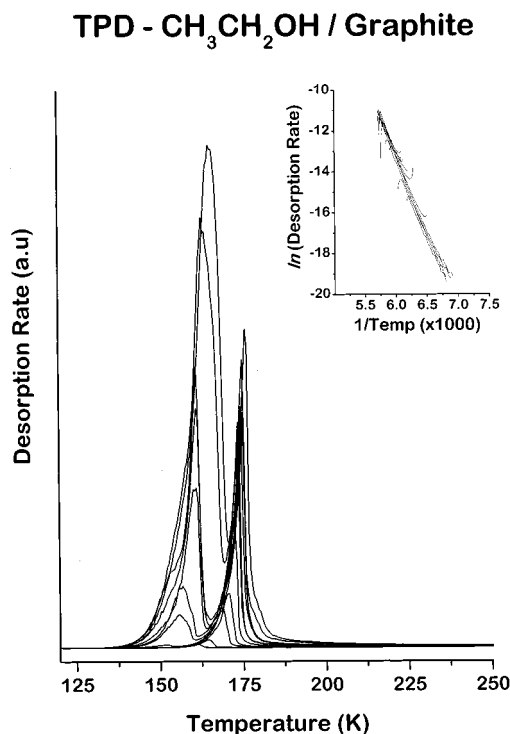


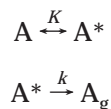
**Figure 5.** Thermal desorption of CH<sub>3</sub>CH<sub>2</sub>OH from the surface of graphite. The initial CH<sub>3</sub>CH<sub>2</sub>OH coverage ranges from <1% to >2 ML. The monolayer and multilayer desorption features are well resolved, although there is some overlap at high coverages. The monolayer peak desorption temperatures increase with increasing coverage. The TPD spectra were collected with a heating rate of 2 K/s while monitoring the signal at  $m/q = 31$ . The inset shows an Arrhenius plot of the leading edges of the monolayer desorption curves. The straight lines indicate that the process is zero-order, and the slopes give a desorption energy of  $\Delta E_{\text{des}} = 57.6 \pm 0.7$  kJ/mol. This is not significantly different from that of CF<sub>3</sub>CH<sub>2</sub>OH.

The desorption kinetics of the CH<sub>3</sub>CH<sub>2</sub>OH multilayer should reflect the energetics of vaporization of bulk ethanol. The value for the desorption energy calculated from the multilayer desorption spectra for CH<sub>3</sub>CH<sub>2</sub>OH is  $\Delta E_{\text{des}}^{\text{mult}} = 46.4 \pm 0.8$  kJ/mol. This can be compared with a number determined from a correlation developed from experimental data for CH<sub>3</sub>CH<sub>2</sub>OH vaporization in the temperature range 298–469 K.<sup>22</sup> At 150 K (the multilayer desorption temperature for CH<sub>3</sub>CH<sub>2</sub>OH) the heat of vaporization of ethanol is estimated to be  $\Delta H_{\text{vap}} = 48.3$  kJ/mol, which is in very close agreement with the value of  $\Delta E_{\text{des}}^{\text{mult}}$  measured in our work.

## 4. Discussion

**4.1. Zero-Order Desorption of Monolayers on Graphite.** One normally expects that the desorption of simple molecular species adsorbed at sub-monolayer coverages should be describable as a first-order process. Nonetheless, it is quite clear that the shapes of the desorption profiles in Figures 2–5 are those of a zero-order process, and the fits of the curves to Arrhenius forms illustrated in the insets certainly confirm this.

The commonly suggested mechanism for apparently zero-order desorption that occurs under conditions for which one expects first-order kinetics is a two-step process. It is proposed that the adsorbed species is present on the surface in the form of islands which are in equilibrium with a two-dimensional gas. It is the molecules in the 2D gas phase that desorb from the surface. This can be described by the two following steps:



In this model A is the species in the condensed 2D islands, A\* is the species in the 2D gas, and A<sub>g</sub> is the species that has irreversibly desorbed into the gas phase or vacuum. The kinetics for the process are first described by an equilibrium step where the coverage of A\* is determined by the equilibrium constant *K* and the concentration of species in the islands [A].

$$\theta_{A^*} = K[A]$$

The desorption step is actually a first-order process that is dependent on the coverage of species in the 2D gas.

$$r_d = k\theta_{A^*}$$

$$= kK[A]$$

Since the concentration of species in the 2D islands is a constant, the net desorption process appears to be zero-order in the adsorbate coverage on the surface. When we analyze the desorption curves using an Arrhenius plot, the  $\Delta E_{\text{des}}$  comes from a combined rate constant *k* and equilibrium constant *K*. This gives the net energy needed to displace the molecules from the 2D islands into the gas phase.

At this point it is probably appropriate to make some comment concerning the pre-exponential factors that have been measured for the desorption of the ethers and alcohols from the graphite surface. These are listed in Table 1 and fall into the range 10<sup>11</sup> to 10<sup>17</sup> s<sup>-1</sup>. It is not uncommon in studies that carefully measure pre-exponential factors for desorption to observe values in this range, although in many studies of desorption kinetics it is commonly assumed that the pre-exponent is of the order of 10<sup>13</sup> s<sup>-1</sup>. An error of 1 order of magnitude in the pre-exponent results in an error of roughly 5% in the predicted desorption energy. One thing that should be pointed out is that the pre-exponent for the process that is being observed in this study is not simply a pre-exponent for elementary desorption. It is the pre-exponent associated with the sequential processes of island evaporation and desorption. In other words the pre-exponent that we measure derives from both the rate constant for desorption, *k*, and the equilibrium constant for island evaporation, *K*. This may account for the range of values observed.

**4.2. Heterogeneity of a-C Films.** One of the primary goals of this work has been to address the issue of heterogeneity in the binding sites for ethers, alcohols, and ultimately Fomblins adsorbed on a-C films. The desorption spectra shown in Figure 1 reveal that the peak desorption temperatures for (CF<sub>3</sub>CF<sub>2</sub>)<sub>2</sub>O on a-CN<sub>x</sub> decrease with increasing coverage and that the peak desorption widths are much greater than those observed on the graphite surface. This is a general observation that applies to all the ethers and alcohols adsorbed on all of the many types of a-C films that we have worked with in the past.<sup>11-16</sup> One of the two possible explanations is that there are repulsive interactions between adsorbed ethers or adsorbed alcohols which lower the net desorption energy as the coverage is increased. This has been observed many times with adsorbates on single-crystalline metal surfaces. The second explanation for the desorption peak widths on a-C is that their surfaces are heterogeneous in the sense that they expose many different types of binding sites for adsorption. At low coverages the adsorbed ethers or

alcohols occupy those sites with the highest adsorption affinities. As the coverage increases, however, these high-affinity sites become saturated and the adsorbing species must occupy sites of decreasing adsorption affinity.

The fact that we observe a zero-order desorption process for the ethers and the alcohols on the graphite surface indicates that the adsorbed species tend to condense into 2D islands on the surface. This must imply that the natural interactions between these adsorbed species are attractive rather than repulsive. The implication is that the true origin of the breadth of the TPD curves on the a-C surfaces is the heterogeneity of their surfaces. Such heterogeneity is not surprising, since it is known that the a-C films are composed of both sp<sup>2</sup> and sp<sup>3</sup> hybridized carbon atoms with varying hydrogen or nitrogen substitution. In addition the surfaces of most of these carbon films are partially oxidized by exposure to air before the application of the lubricant.<sup>15,21</sup> In previous work we have used the coverage dependence of the (CF<sub>3</sub>CF<sub>2</sub>)<sub>2</sub>O and CF<sub>3</sub>CH<sub>2</sub>OH desorption curves to map out the distribution of binding site affinities on the surfaces of a-CH<sub>x</sub>, a-CN<sub>x</sub>, and DLC films.<sup>15</sup> Although they do not differ greatly from one film to the next, the range of desorption energies on a given film can be quite broad. For (CF<sub>3</sub>CF<sub>2</sub>)<sub>2</sub>O the desorption energy at low coverages is  $\Delta E_{\text{des}} \sim 45$  kJ/mol and drops to  $\Delta E_{\text{des}} \sim 30$  kJ/mol as the coverage approaches a monolayer. In the case of CF<sub>3</sub>CH<sub>2</sub>OH the desorption energy is higher and ranges from  $\Delta E_{\text{des}} \sim 57$  to 40 kJ/mol as the coverage varies from zero to saturation of the monolayer. These desorption energies that have been measured in this work on graphite are  $\Delta E_{\text{des}} = 32.5 \pm 0.9$  kJ/mol for (CF<sub>3</sub>CF<sub>2</sub>)<sub>2</sub>O and  $\Delta E_{\text{des}} = 55.9 \pm 0.9$  kJ/mol for CF<sub>3</sub>CH<sub>2</sub>OH.

**4.3. Interactions of Fluoroethers with Graphite and a-C Films.** The previous studies of ether adsorption on the surfaces of a-C films have compared the desorption energies of fluorinated ethers with those of their hydrocarbon analogues in order to probe the nature of the interactions of the ethers with the surface. In all ethers and on all carbon films we have observed that the desorption energy of the hydrocarbon ether is greater than that of its fluorinated analogue.<sup>11-13</sup> In other words, fluorination weakens the interaction of the ether with the surface. This has also been observed on the surfaces of a number of metals.<sup>18-20</sup> Comparison of the desorption energies of the ethers on the graphite surface reveals that (CF<sub>3</sub>CF<sub>2</sub>)<sub>2</sub>O ( $\Delta E_{\text{des}} = 32.5 \pm 0.9$  kJ/mol) is much more weakly bonded to the surface than (CH<sub>3</sub>CH<sub>2</sub>)<sub>2</sub>O ( $\Delta E_{\text{des}} = 45.4 \pm 1.8$  kJ/mol). The interpretation is that the interaction with the surface occurs through electron donation from the lone pairs on the oxygen atoms. The highly inductive character of the fluoroethyl groups weakens this interaction and thus lowers the desorption energy of (CF<sub>3</sub>CF<sub>2</sub>)<sub>2</sub>O compared to (CH<sub>3</sub>CH<sub>2</sub>)<sub>2</sub>O.

**4.4. Interactions of Fluoro Alcohols with Graphite and a-C Films.** Comparison of the desorption energies of alcohols and fluorinated alcohols on the a-C films has revealed that fluorination increases the strength of the interaction with the surface. In other words the desorption energy of CF<sub>3</sub>CH<sub>2</sub>OH is higher than that of CH<sub>3</sub>CH<sub>2</sub>OH.<sup>13-16</sup> On the a-C films the difference in the desorption energies at low coverage is roughly 6 kJ/mol. The interpretation of this effect is that the alcohols interact with the surface through hydrogen bonding. In essence this is a proton donation mechanism and is opposite in nature to the electron donation mechanism of ether adsorption. As a result, fluorination of the alcohols strengthens rather than weakens the interaction with the a-C surfaces. The case on the graphite surface is different. The desorption energies are  $\Delta E_{\text{des}} = 55.9 \pm 0.9$  kJ/mol for

$\text{CF}_3\text{CH}_2\text{OH}$  and  $\Delta E_{\text{des}} = 57.6 \pm 0.7$  kJ/mol for  $\text{CH}_3\text{CH}_2\text{OH}$ , respectively. These are not significantly different from one another. There are significant differences between the graphite and a-C surfaces that can account for the differences in the nature of the bonding of the alcohols to these surfaces. If the interaction of the alcohols with the a-C surface occurs through hydrogen bonding, then there must be some proton acceptor sites on the surface. The most probable sites are the oxygenated species such as C(=O) or COC linkages that are known to exist as a result of the exposure of these surfaces to air.<sup>15,21</sup> The graphite surface is purely  $\text{sp}^2$  carbon and has no oxygen and therefore no proton acceptor sites at which the alcohols can adsorb through hydrogen bonding. Thus, the interaction between the alcohols and the graphite surface is probably quite different than that observed on the a-C surfaces. The other mechanism that might be considered for bonding of the alcohols to the graphite surface would be one of electron donation from the lone pairs of the oxygen atom. This is the same mechanism as is observed for the ethers on the graphite and a-C surfaces. In the case of the alcohols, one does not observe that fluorination of the methyl group decreases the desorption energy, as is observed in the case of the diethyl ethers; however, this may simply be due to the fact that fluorination occurs at the  $\beta$ -carbon in  $\text{CF}_3\text{CH}_2\text{OH}$  rather than the  $\alpha$ -carbon, as occurs in  $(\text{CF}_3\text{CF}_2)_2\text{O}$ . As a result, the inductive substituent effect of the fluorine will have much less effect on electron

donation in the alcohols than in the ethers. This argument is somewhat speculative but would explain the lack of fluorine substituent effects on the bonding of the alcohols to the graphite surface.

## 5. Conclusions

The desorption spectra of ethers and alcohols from the surface of graphite clearly show that the natural interactions between these molecules are attractive in nature. On the graphite surface these interactions lead to the coalescence of the adsorbate layer into islands. These observations imply that the coverage dependence of the desorption energies of the ethers and alcohols on the surfaces of a-C films results from heterogeneity of the film surface. These carbon films expose a variety of sites with varying affinities for adsorption of the ethers and alcohols. As such they represent a very complex environment for the adsorption of lubricants such as Fomblin Zdol.

**Acknowledgment.** This work has been supported with funds from Seagate Technology, the National Storage Industries Consortium, and also the Data Storage System Center of Carnegie Mellon University through Grant No. ECD-8907068 from the National Science Foundation.

LA001397N